Talanta Open 7 (2023) 100236

Contents lists available at ScienceDirect

Talanta Open

journal homepage: www.sciencedirect.com/journal/talanta-open

Bright, green fluorescent carbon dots for sensitive and selective detection of ferrous ions

Allora McEnroe [a], Eric Brunt [a], Nazanin Mosleh [a], Jason Yu [a], Richard Hailstone [b], Xiangcheng Sun [a,*]

[a] Department of Chemical Engineering, Rochester Institute of Technology, Rochester, New York, 14623, United States
[b] Center for Imaging Science, Rochester Institute of Technology, Rochester, New York, 14623, United States

ARTICLE INFO

Keywords:
Green fluorescent carbon dots
Ferrous ions
Sensitive and selective detection
Quenching mechanism

ABSTRACT

Iron is critical to living organisms; excess or lack of iron could lead to a series of diseases. In this work, fluorescent carbon dots were developed as an efficient probe for sensitive and selective detection of ferrous ions (Fe^{2+}). We reported on simple and one-pot synthesis of uniform, bright, and green fluorescent carbon dots with aqueous stability in a wide pH range. The formation of green fluorescence is attributed to the doping of nitrogen into carbon materials. The as-synthesized carbon dots demonstrated wavelength-independent emission properties. Fluorescence of carbon dots was quenched efficiently, sensitively and selectively by ferrous ions over a series of other common metal ions and anions, with a detection limit of 16 μM, and a wide detection range of 0.033 -1.044 mM. Efficient quenching of carbon dots could be explained by the efficient binding of ferrous ions on carbon dots surface. Aggregation caused quenching was later proposed and verified as the quenching mechanism of carbon dots toward ferrous ions. The developed carbon dots show great promise in the development of efficient sensors and adsorbents for ferrous ions.

1. Introduction

Iron, an important participant in many biological metabolic processes, is critical to the survival of living organisms [1]. Iron deficiency or overload causes several diseases in human beings [2,3]. It is recommended to even give infants iron supplements daily or to directly feed iron fortified formula, and to screen babies for iron deficiency (anemia) [4]. On the other hand, steel corrosion of distribution pipes could lead to the metal (iron) contamination in drinking water [5]. This has led to the Environmental Protection Agency (EPA) set the secondary standard for iron in drinking water as 0.3 mg/L.

Carbon dots (CDs), also called as carbon nanoparticles, were discovered in 2004 accidently via the separation and purification of arc-discharged synthesized carbon nanotubes [6]. Since then, carbon dots have grown as one novel fluorescent material due to the simple synthesis, excellent optical properties, good photo-stability, and low-cytotoxicity [7,8]. The optical properties of carbon dots were extensively utilized for a variety of applications for sensing, bio-imaging and drug-delivery, light-emitting devices, etc. [9]. Taking advantage of their fluorescent properties, the detection of a series of targets has been achieved, such as, cations, anions, small molecules, macromolecules, cells and bacteria [10]. Most carbon dots for sensing show blue fluorescence emission colors or longer emissions with low quantum yields [11,12]. Active efforts have been reported to obtain carbon dots with bright long wavelength emission, and have usually involved complex synthesis, toxic components or cumbersome post-synthesis purification [13–17]. Here we show simple and one-pot synthesis, systematic characterization and application of bright green carbon dots.

Many research groups reported the detection of ferric (Fe^{3+}) ions using fluorescent carbon dots due to the significance of iron, however, efficient probes to detect ferrous (Fe^{2+}) ions sensitively and selectively was less explored [10,18,19]. As a trace element, ferrous ions play an important role in biological and environmental system [20]. Catalyzed by ferrous ions, reactive oxygen species are generated and enhance the oxidative stress [21–23]. This could induce biochemical signaling processes and decline in mitochondrial activity, and promote the occurrence of degenerative diseases. Detection of ferrous ions could also be an early diagnosis and prevention of steel corrosion [24]. Monitoring of ferrous cations was recently applied for investigating anodic oxidation for corrosion processes [25]. Therefore, it is necessary to develop a

* Corresponding author.
E-mail address: xgsche@rit.edu (X. Sun).

https://doi.org/10.1016/j.talo.2023.100236
Received 24 March 2023; Received in revised form 19 May 2023; Accepted 22 May 2023
Available online 23 May 2023

sensitive, convenient and cheap probe for ferrous iron detection in aqueous conditions and organisms, considering the practical significance.

In this work, we reported a simple, one-pot, hydrothermal synthesis of green fluorescent carbon dots for sensitive and selective detection of ferrous ions. The obtained carbon dots showed excitation-independent properties with an emission peak at ~ 510 nm without obvious shift. The carbon dots also showed stability at high ionic strength, and pH dependent properties. The fluorescence of carbon dots in aqueous solutions could be quenched by addition of ferrous ions, with a wide range from 0.033 to 1.044 mM, producing an immediate change in intensity. The carbon dots also demonstrated good selectivity over a series of other cations/anions, and especially ferric ions. The sensing mechanisms were explained by the aggregation induced quenching, verified by with sizes distribution of CDs upon interactions with iron ions through dynamic light scattering (DLS) and aggregated TEM images. The work here provides one potential probe for efficient determination of ferrous ions and extends to be used in organisms, for possible bio/chemical sensing applications of ferrous ions, as well as a good adsorbent for ferrous ions.

2. Experimental

2.1. Reagents and chemicals

All reagents and chemicals were of analytical reagent grade or higher quality, purchased and used without further purification. m-phenylenediamine flakes (99%) and ethylenediamine (≥ 99%) used for the synthesis of the CDs were bought from Sigma Aldrich. Metal ions and anions for the sensing experiments were obtained from Fisher Chemical, Alfa Aesar, Acros Organics, or VWR. Salts were used such as ferrous sulfate heptahydrate, iron (III) citrate hydrate, nickle (II) chloride hexahydrate, manganese(II) sulfate monohydrate, zinc sulfate heptahydrate, magnesium chloride hexahydrate, potassium chloride, ammonium chloride and sodium chloride. pH buffer solutions were prepared in water using chemicals such as sodium bicarbonate, sodium carbonate, sodium phosphate monobasic dihydrate, sodium phosphate dibasic, and citric acid supplied from Sigma Aldrich. Ultrapure water (>=18.2 MΩ·cm) was used to prepare solutions if without other notification.

2.2. Synthesis of fluorescent carbon dots

80 mg (0.74 mmol) m-phenylenediamine and 44.8 mg (0.74 mmol) ethylenediamine were dissolved in 2 mL of water in ambient conditions. The solution was transferred into a 20 mL Teflon lined autoclave reactor and hydrothermally heated for three hours at 150 °C. The CDs solution was obtained and then centrifuged at 12,000 rpm for 15 min to remove large particles. The supernatants CDs solution were then diluted 500 times for further sensing studies without further purification.

2.3. Characterization

The absorption spectra was recorded on a UV–Vis spectrophotometer using a UV-2600 unit by Shimadzu. The florescence emission and excitation spectra were obtained using a Cary Eclipse florescence spectrophotometer by Agilent Technologies. A high resolution transmission electron microscope (HRTEM, JEOL JEM-2010) at an operating voltage of 200 kV was used to observe the morphology and size of the CDs. The X-ray diffraction patterns of CDs operating at 40 kV and 40 mA were obtained using Bruker D8 XRD instrument. The Fourier transform infrared (FTIR) spectra were collected using an IRAffinity-1 Shimadzu spectrophotometer with a Miracle single reflection horizontal ATR accessory. To collect X-ray photoelectron spectra (XPS) of the samples, a Thermo Scientific Nexsa XPS Spectrometer using a monochromatic Al Kα X-ray source (1486.6 eV) was employed. A pass energy of 200 eV for survey spectra and 50 eV for high resolution spectra were used. Raman spectrum of CDs were obtained in Bruker- Senterra II under 633 nm. Dynamic light scattering and Zeta potential measurements were performed with a Brookhaven Nanobrook Omni analyzer (λ=640 nm).

2.4. Quantum yield (QY) measurements

The quantum yield of the fluorescent CDs was calculated using the reference fluorophore fluorescein, dissolved in 0.1 M NaOH with a known quantum yield of 95%. Utilizing the following equation [12,26]:

$$QY_C = QY_R \frac{F_C}{F_R} \frac{OD_R}{OD_C} \frac{n_C^2}{n_R^2} \quad (1)$$

The subscripts R and C refer to the reference fluorophore and the CDs, respectively. QY is the quantum yield, F is integrated florescent intensity of the emission peak, OD is the optical density of the samples at the excitation wavelength, and n is the refractive index of the solutions.

2.5. Detection of ions in aqueous solutions

The concentrations of ferrous ions are correlated with the emission fluorescence intensity of CDs, showing that with the addition of Fe^{2+} the CDs exhibit quenching behavior. The CDs were tested against various concentrations of ferrous to examine the quenching behavior. 3 mL of the diluted CDs in pH 7 buffer solutions (0.01 M) in deionized water were added into cuvettes, which were then exposed to incremental additions of various ions at room temperature. The CDs were excited at 415 nm over an emission range of 450 nm – 700 nm. Different cations/anions were used instead of ferrous ions for selectivity study. The quenching efficiency (QE) was then calculated utilizing the following equation:

$$QE = (I_0 - I)/I_0 \quad (2)$$

QE is the quenching efficiency, I_0 is the initial fluorescence intensity at 510 nm without the addition of any analytes, and I is the corresponding fluorescence intensity in the presence of various concentrations of different ions.

2.6. Mechanisms studies on fluorescence quenching of carbon dots toward ferrous ions

After addition of ferrous ions into carbon dots solutions, we observed the precipitation of carbon dots, probably due to efficient binding of ferrous cations onto CDs surfaces. The binding causes aggregation of CDs in the solution, which results in fluorescence quenching. In order to verify the mechanism of aggregation induced quenching, we measured the size distribution of CDs-ferrous mixtures through dynamic light scattering and collected TEM images. As a control, we conducted experiments using carbon dots and ferric ions mixtures.

3. Results and discussions

3.1. Characterization of carbon dots

High resolution transmission electron microscope was used to image the size and morphology of formed dots. Well-dispersed uniform carbon dots were observed, with diameters in the range of 3.5 ± 0.7 nm (Fig. 1A). The size distribution of these nanodots is presented in Fig. 1B. From the HRTEM images, carbon dots particles were observed to be amporphous, and few particles possessed well-resolved lattice fringes. Dynamic light scattering results also gave the size distribution of carbon dots in aqueous solutions, with the size of ~ 4.1 nm (Figure S1), which are consistent with TEM results. As shown in Fig. 1C, the CDs exhibited a broad diffraction peak at $2\theta = 20°$, which matched to the (002) plane of the graphite structure, indicating the carbon crystals was small and had a disordered lattice arrangement to some extent [27]. Raman spectra of CDs were obtained, while D-band (~ 1340 cm^{-1}) or G-band (~ 1560

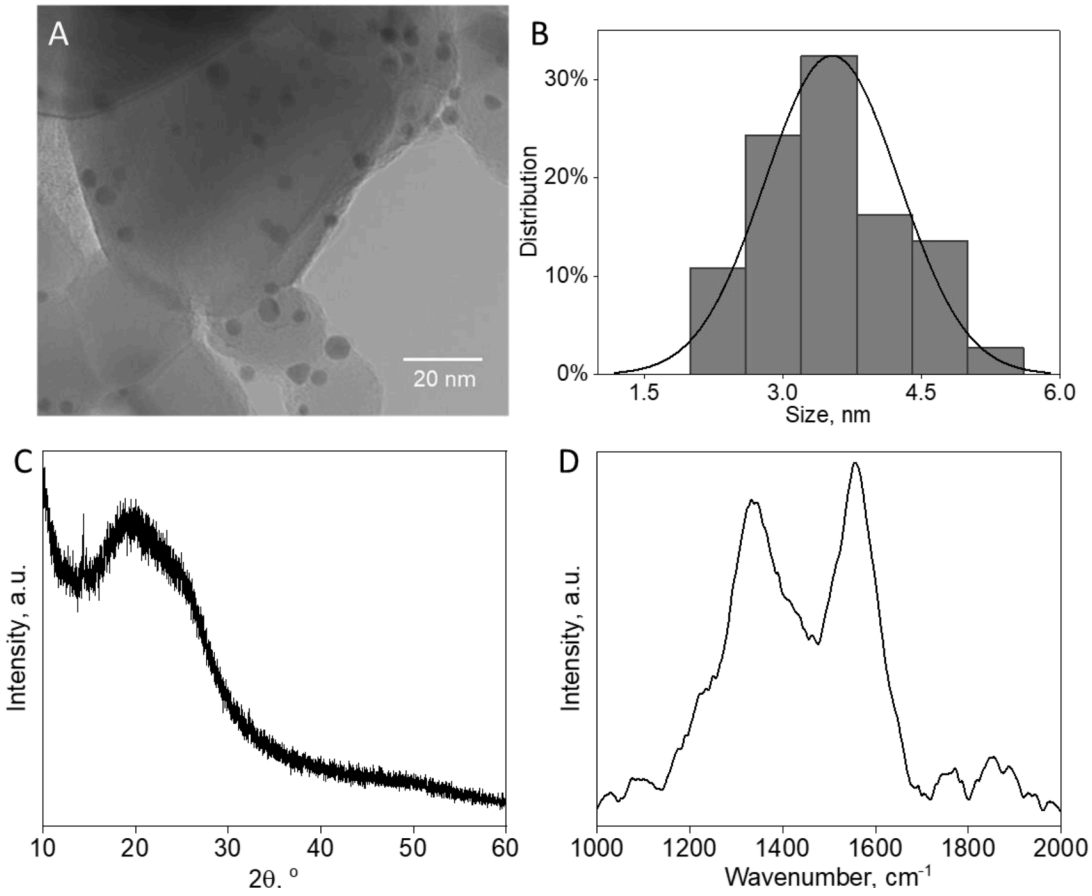

Fig. 1. A) HR-TEM images of obtained carbon dots. B) Size distribution of carbon dots from TEM graph. C) XRD pattern of the obtained carbon dots; D) Raman spectrum of the carbon dots.

cm^{-1}) were observed (Fig. 1D), suggesting disordered structures and graphitic structures, respectively of carbon materials [17]. A high ratio of I_D/I_G of about 1.35 and amorphous structures of carbon dots could be related to the red shift of CDs emissions and formation of green emissions [28].

FTIR was applied to characterize the composition and functional

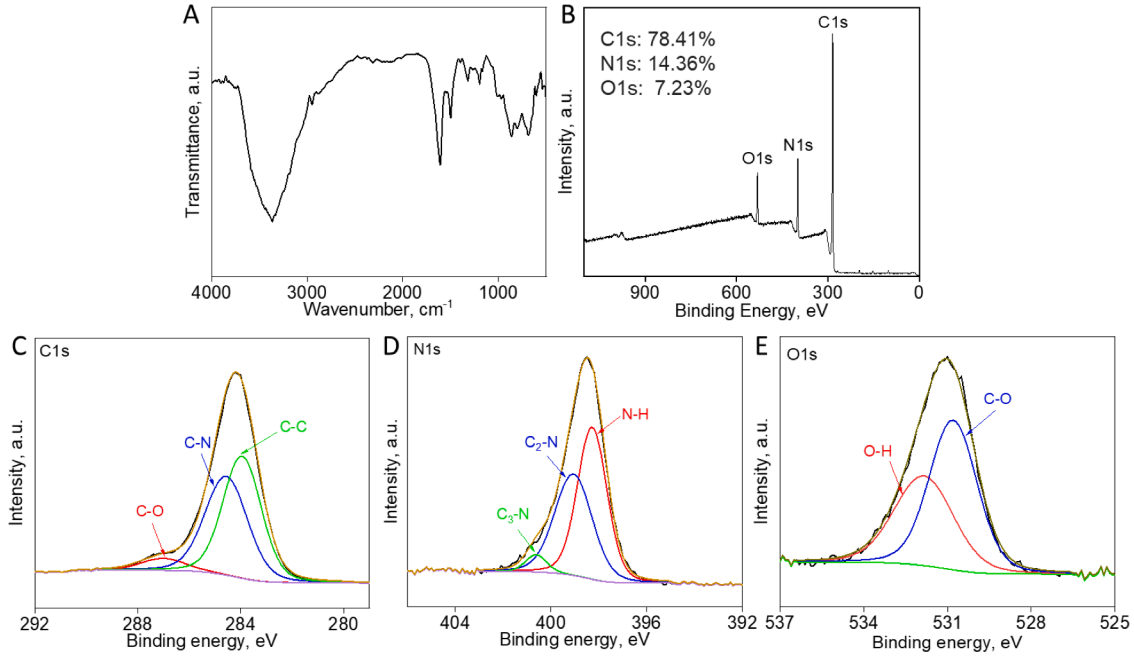

Fig. 2. FTIR and XPS spectra of carbon dots. A) FTIR spectrum of the synthesized carbon dots; B-D) XPS spectra of the carbon dots. B) XPS survey spectrum. High resolution XPS spectra of the C 1 s (C), N 1 s (D) and O 1 s (E) lines, in black, including their fitted peaks.

groups of carbon dots. As shown in Fig. 2A, a broad peak at 3365 cm^{-1} corresponds to the stretching vibrations of N—H groups and O—H groups. A peak at 2954 cm^{-1} is corresponding to C—H groups, and peaks at 1604 cm^{-1} and at 1497 cm^{-1} are attributed to the stretching vibration of C = C [3,17]. A peak at 1397 cm^{-1} corresponds to C—NH—C groups, and peaks at 1195 cm^{-1}, 1072 cm^{-1} and 1010 cm^{-1} can be assigned to C—N/C—O groups. The stretching vibration of N—H groups can be found at 900 cm^{-1} [29]. The results indicate the presence of NH_2 groups on the carbon dots surface, which may endow a positive charge to the carbon dots, and this was further verified by Zeta potential of the carbon dots as 9.32 mV. The zeta potential also suggests the stability of carbon dots.

X-ray photoelectron spectroscopy (XPS) analysis was further used to investigate the surface of the carbon dots. The XPS survey spectrum of the carbon dots is presented in Fig. 2B, showing the carbon dots are mainly composed of carbon (78.41%), nitrogen (14.36%) and oxygen (7.23%). The presence of oxygen in the carbon dots is not surprising, probably due to the solvent or an environmental effect. Similarly, the presence of oxygen in the carbon dots was observed even using precursors without oxygen [15]. The high resolution C1s spectrum was collected and shown in Fig. 2C. The spectrum exhibits 3 main peaks, the binding energy peaks at 283.9 eV, 284.6 eV and 287.0 eV, which could be assigned to carbon in the form of C-C, C-N, and C-O, respectively [30]. Graphite-like, pyridinic/pyrrolic-like and N—H groups could be assigned by the high resolution N1s spectrum (Fig. 2D) at 400.6 eV, 399.1 eV, and 398.3 eV. High resolution O1s spectrum (Fig. 2E) indicates the presence of C—O and O—H groups. This verifies that the successful formation of nitrogen doped carbon dots.

3.2. Optical properties of carbon dots

m-phenylenediamine and ethylenediamine condensation reactions under hydrothermal conditions formed the green fluorescent carbon dots. The green fluorescence was attributed to the doping of nitrogen into carbon nanoparticles. In order to verify the effect of nitrogen doping for formation of green fluorescence of carbon dots, we prepared carbon dots using m-phenylenediamine as a single precursor at similar hydrothermal conditions. We found blue fluorescence of carbon dots were generated (Supplementary Figure S2), and the results were consistent with the previous report, where using m-phenylenediamine as a single precursor in hydrothermal conditions for creating blue fluorescent carbon dots [15]. Therefore, using dual precursors of m-phenlenediamine and ethylenediamines generated green fluorescent carbon dots, and the use of ethylenediamine promoted shifting carbon dots emissions into longer wavelength.

Absorption spectra at ~ 290 nm, corresponding to the π-π* transitions of C = C and C = N bonds, in the aromatic rings, which does not typically generate fluorescence. However, in the lower-energy region, the peak at ~ 410 nm were also observed, indicated the extended conjugation (aromatic) structures or presence of surface states. The fluorescence emission spectra excited at 415 nm is shown in Fig. 3A, and an emission peak at ~ 510 nm was observed, indicating the formation of green fluorescent carbon dots. Consistent with the green emission color of carbon dots in solution under UV (365 nm) irradiation, and the inset of Fig. 3 shows the images of carbon dots solutions with pale yellow and green colors under visible light and 365 nm light, respectively. An excitation spectrum of the carbon dots using emission wavelength of 510 nm was obtained, and several peaks at ~ 415 nm and 260 nm, are similar to that of the absorption spectrum of the carbon dots, showing the presence of two major chromophores in carbon dots. Quantum yield of carbon dots in water as high as 22.5% was obtained using Eq. (1) (detail in Supplementary Figure S3), which is higher than or comparable to previous reported green fluorescent carbon dots [11,15,31-33].

Contrary to many other reported CDs, the emission peak of our CDs did not shift noticeably when excitation wavelength changed, and emission peaks centered at ~ 510 nm were observed (Fig. 3B), which is consistent with the emission photos with green colors under varying excitation wavelengths (Figure S4 in the supporting information). The excitation-independent emission properties could be attributed to the uniformity of the as-synthesized carbon dots and less defects on the carbon dots surface. The photoluminescence emission clearly originated from the absorption in the lower-energy region, and the excitation at 415 nm generated the highest fluorescence intensity, which are consistent with the peak in the excitation and absorption spectra. The minimum fluorescence was observed when excited at shorter wavelengths (Supplementary Figure S5, Excited from 255 – 335 nm).

The emission properties of the carbon dots diluted in pH buffer solutions was investigated and the fluorescent intensities vs pH are shown in Fig. 4A. In strong acidic conditions (pH 3–5), the fluorescence intensity increased with increasing pH of solutions, further increase of pH (5–11), the CDs emission intensity did not change obviously. The obtained carbon dots showed pH dependent properties only in acidic environments, but no obvious change in basic conditions, which are different from our previous reports [11,12]. The amines on the surface serve as Lewis base, reacted with acid to form ammonium salt and affect the surface state of carbon dots, and thus the fluorescence was quenched in strong acidic conditions. In addition, the stability of carbon dots in presence of various concentrations of NaCl was studied, and fluorescence intensity remains almost unchanged from 0 to 2 molar concentrations (Fig. 4B). The high stability of carbon dots in aqueous solutions is attributed to the functional groups on the surface and the mild positively charge (Zeta potential of 9.32 mV). The results suggests the

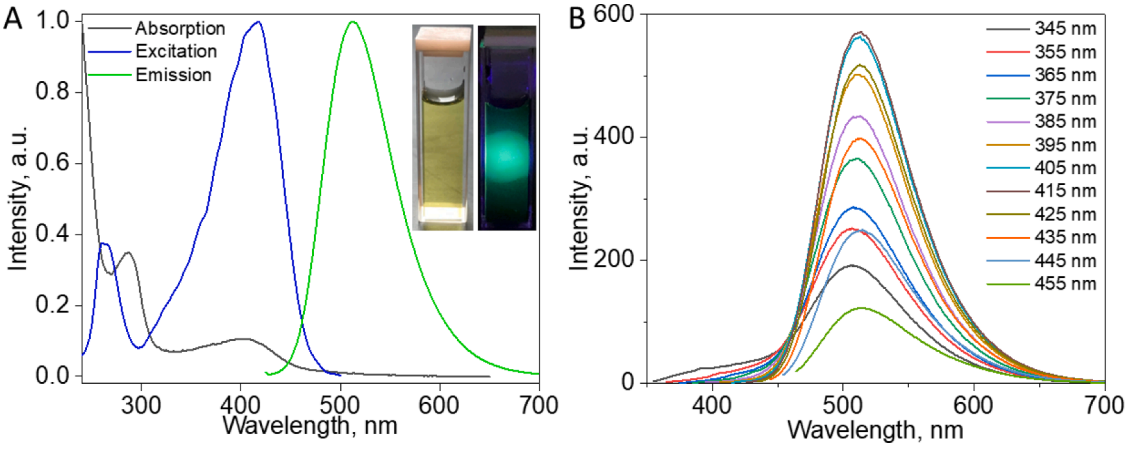

Fig. 3. A) Normalized UV–vis absorption, excitation and emission spectra of the carbon dots in aqueous solution. B) Emission spectra of the carbon dots solution with varying excitation wavelengths over the range of 345 nm – 455 nm.

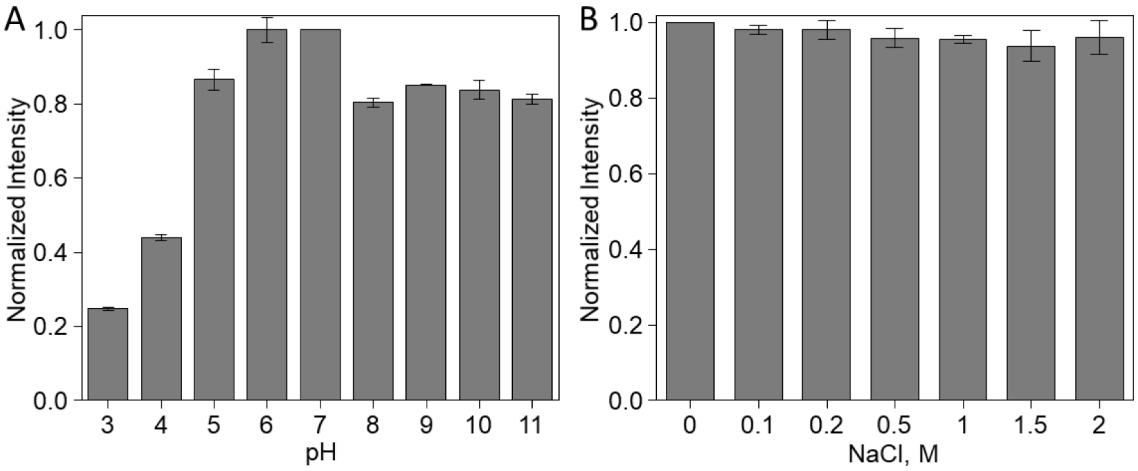

Fig. 4. A) pH and B) salt effect on the fluorescent intensity of the carbon dots in aqueous solutions.

obtained carbon dots could be potentially used for pH sensing and in high ionic conditions.

3.3. Detection of ferrous ions in aqueous solution

It is essential to detect ferrous ions in aqueous solution due to the important and practical relevance in health and the environment. We firstly conducted the fluorescence titration experiments by incremental addition of ferrous solutions in the CDs solution and then collected the fluorescence spectra in presence of various concentrations of ferrous ions. As presented in Fig. 5A, the fluorescence intensities gradually quenched as the ferrous concentrations increased. The limit of detection to ferrous ions could be reached at 16 μM, by using the 3σ/k, where σ is the standard deviation and k is the slope.

The quenching results could be quantitatively explained by the Stern-Volmer equation:

$$I_0/I = 1 + K_{SV}[A] \quad (3)$$

I_0 is the initial fluorescence intensity at 510 nm, I is the corresponding intensity in presence of ferrous analyte, [A] is the molar concentration of the analyte, and K_{SV} in M^{-1} is the quenching constant. A non-linear fitting could be observed, even in a low concentration range, a good linear fitting can't be obtained (Fig. 5B). A non-linear behavior could be due to the presence of both static quenching and dynamic quenching [26]. As shown in Fig. 5B, a modified Stern-Volmer equation can be used as follows,

$$I_0/I = (1 + K_S[A])(1 + K_D[A]) \quad (4)$$

where K_S and K_D are the Stern-Volmer constants for the static and dynamic quenching, respectively. Thus a second order polynomial was used to fit the quenching results. We found the results could be fitted for the equation very well. Therefore, both static quenching and dynamic quenching are responsible for the CDs fluorescence quenching induced by ferrous cations.

For a reliable sensor, not only good sensitivity, but also having high selectivity to the analyte is necessary and essential in real applications. We then investigated the quenching performance by a series of common metal ions and anions. It was found under the same concentration of 0.506 mM, quenching efficiency by Fe^{2+} reached nearly 50%, which was around or greater than 10 times of quenching efficiency induced by a series of other cations or anions (Fig. 6A). Especially, the developed carbon dots probe showed good selectivity to ferrous over ferric ions. Unlike many reported carbon dots for ferric iron and/or total iron detection (as shown in Table 1), the monitoring of ferrous ions by using fluorescent carbon dots are much less explored, and among these very few ones achieved ferrous ions detection with good selectivity over ferric ions. Our current work thus represents one of few studies that achieved ferrous detection with good sensitivity, high selectivity and a broad detection range. Moreover, almost all the carbon dots utilized for iron detection with blue fluorescence, which limits the applications in organisms due to the well-known auto-fluorescence.

In addition, the detection of ferrous in real water using fluorescent

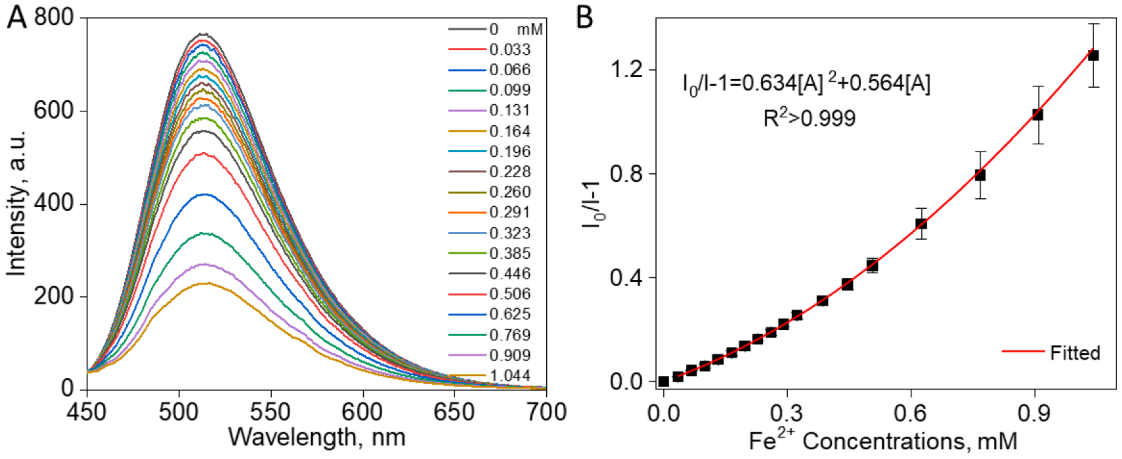

Fig. 5. A) Fluorescence spectra of the carbon dots upon addition of various ferrous concentrations in aqueous solutions. B) Stern-Volmer plot for carbon dots fluorescence quenching by Fe^{2+}, and the fitting with a quadratic equation.

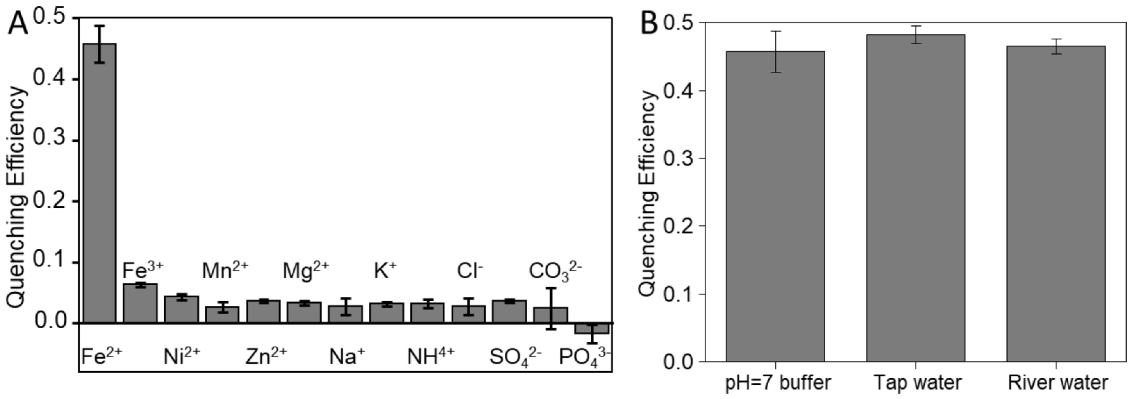

Fig. 6. A) Fluorescence quenching efficiency for the carbon dot sensor upon addition of 0.506 mM of different cations and anions, showing good selectivity toward ferrous ions. B) Fluorescence quenching efficiency for the carbon dots in buffer solution and real water with spiked 0.506 mM of ferrous ions.

Table 1
Recent reports on carbon dots probe for ferrous detection and their properties.

Ref.	CDs color	Limit of detection	Detection range	Selectivity	Quantum yield
[34], 2016	blue	20 nM	0–32 μM	No	10%
[35], 2017	blue/green	60 nM	0.5 – 2 μM	YES	2.3%
[36], 2018	blue	21.9 μM	10–50 μM	Yes	11%
[2], 2019	blue	160 nM	0–300 μM	No	12.2%
[20], 2020	blue	14 μM	25–500 μM	N.A.	N.A.
[37], 2020	Blue	17 nM	0.05–1.5 μM	No	16.8%
[38], 2020	Blue	11 μM	9–60 μM	N.A.	18.2%
[39], 2020	yellow	2.97 μM	15–50 μM	No	25.3%
[27], 2020	blue	51 nM	10–100 μM	No	N.A.
[19], 2022	blue	0.7 μM	0–50 μM	Yes	N.A.
This study	green	16 μM	0.033–1.044 mM	Yes	22.5%

carbon dots was studied. Fig. 6B depicts the comparison of the quenching efficiencies of Fe^{2+}at 0.506 mM to the fluorescence emission of diluted carbon dots in pH 7 buffer in DI water, and spiked in tap water (RIT) and river water (Genesee River, Rochester, NY). As expected, the quenching efficiencies of ferrous in DI water and real water from two different source are nearly overlapped. The differences are less than 6%, which suggests that the matrix effect of real water is negligible. This result indicates that the as-synthesized carbon dot is a good candidate for real sensing applications.

3.4. *Quenching mechanism of CDs toward ferrous ions (Fe^{2+})*

When we gradually added Fe^{2+} cations into carbon dots solutions for titration experiments, we noticed clear precipitation formed in the solution (Supplementary Figure S6). No similar phenomena was observed for other cations. The presence of Fe^{2+} results in a change of CDs' surface chemistry via efficient chelation, due to the coordinate bond formation between ferrous ions and N atoms in functional groups on the surface of CDs [40,41]. We propose Fe^{2+} inducing aggregation of carbon dots results in fluorescence quenching.

In order to verify the aggregation of CDs in presence of Fe^{2+}, DLS was performed to measure the particle sizes [35]. Upon interaction of CDs with 196 μM of Fe^{2+}, the mean particle size was determined to be ~ 200 nm (Fig. 7). In addition, in the CDs-Fe^{2+} mixture, there was a tail of much larger particles with ~ 860 nm, consistent with the formation of large visible particles. We also observed aggregated CDs upon interaction with ferrous ions in the HR-TEM images (Supplementary Figure S7). The results supports that the fluorescence quenching may be mainly due to the aggregation of particles and formation of a weak-binding nonfluorescent complex between Fe^{2+} ions and CDs [42,43]. When Fe^{3+} was added into carbon dots solution, we didn't see clear visible precipitation. The size distribution of CDs with 196 μM of Fe^{3+} was measured through DLS, and the average hydrodynamic diameter of

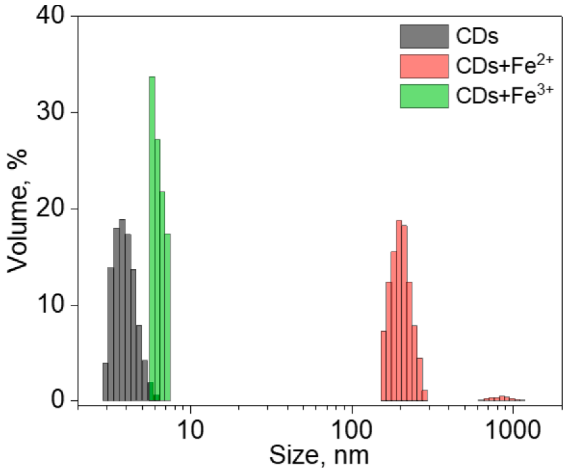

Fig. 7. Sensing mechanism of CDs towards ferrous ions. The histogram of DLS spectra of particle size distributions for CDs, CDs-Fe^{2+}, and CDs-Fe^{3+} (with the iron concentration of 196 μM).

carbon dots increased to 5.8 nm with a very small extent from ~ 4.1 nm of pure CDs. This shows no significant aggregations between CDs and Fe^{3+}, and explains well the good selectivity of CDs probe toward Fe^{2+} over Fe^{3+}. The results indicate that a high amount of ferrous cations bounded to carbon dots surfaces and precipitated out. The observations also suggest that CDs could adsorb Fe^{2+} efficiently due to the special functional groups on the surface. The obtained carbon dots could thus be developed as one chemical probe to detect ferrous cations and one efficient and potential adsorbent to remove ferrous ions in the environment simultaneously.

4. Conclusions

Through simple one-pot hydrothermal synthesis, we obtained nitrogen-doped uniform fluorescent carbon dots. This process generated bright green fluorescence centered at 510 nm for its emission spectra and possessed a 25.5% quantum yield. The carbon dots showed excitation independent emission properties and good aqueous stability in a wide range of pH and strong ionic conditions. The fluorescence signals of carbon dots could be significantly quenched with the addition of Fe^{2+}, thus the CDs could serve as an efficient probe for ferrous ions detection. In addition, the carbon dots showed good selectivity to Fe^{2+} detection over a series of other ions (especially ferric). The quenching behavior is attributed to efficient binding of ferrous ions on CDs surface, and further aggregation of carbon dots. The aggregation induced quenching was verified by the size distribution of CDs and aggregated ones upon interaction with iron cations. The as-synthesized carbon dots provide high potential in use as an efficient probe for ferrous detection and as a good adsorbent for removal of the ferrous cation in the environment.

CRediT authorship contribution statement

Allora McEnroe: Methodology, Investigation, Formal analysis. **Eric Brunt:** Investigation, Validation. **Nazanin Mosleh:** Investigation, Methodology, Validation. **Jason Yu:** Investigation. **Richard Hailstone:** Investigation, Formal Analysis, Article proofreading. **Xiangcheng Sun:** Conceptualization, Formal Analysis, Writing, Supervision, Funding Acquisition.

Declaration of Competing Interest

The authors declare that they have no known competing financial interests or personal relationships that could have appeared to influence the work reported in this paper.

Data availability

Data will be made available on request.

Acknowledgments

X.C. Sun would like to thank the start-up fund from the Rochester Institute of Technology (RIT). We acknowledge Dr. John Wright from Cornell University for helpful discussions. This work made use of the Cornell Center for Materials Research Shared Facilities which are supported through the NSF MRSEC program (DMR-1719875).

Supplementary materials

Supplementary material associated with this article can be found, in the online version, at doi:10.1016/j.talo.2023.100236.

References

[1] J. Kaplan, D.M. Ward, The Essential Nature of Iron Usage and Regulation, Curr. Biol. 23 (15) (2013) R642–R646, https://doi.org/10.1016/j.cub.2013.05.033.
[2] G. Liu, B. Li, Y. Liu, Y. Feng, D. Jia, Y. Zhou, Rapid and High Yield Synthesis of Carbon Dots with Chelating Ability Derived from Acrylamide/Chitosan for Selective Detection of Ferrous Ions, Appl. Surf. Sci. 487 (2019) 1167–1175, https://doi.org/10.1016/j.apsusc.2019.05.069.
[3] X.-Y. Zhang, Y. Li, Y.-Y. Wang, X.-Y. Liu, F.-L. Jiang, Y. Liu, P. Jiang, Nitrogen and sulfur Co-doped carbon dots with bright fluorescence for intracellular detection of iron ion and thiol, J. Colloid Interface Sci. 611 (2022) 255–264, https://doi.org/10.1016/j.jcis.2021.12.069.
[4] T.O. Scholl, Iron status during pregnancy: setting the stage for mother and infant, Am. J. Clin. Nutr. 81 (5) (2005) 1218S–1222S, https://doi.org/10.1093/ajcn/81.5.1218.
[5] I.A. Alam, M. Sadiq, Metal contamination of drinking water from corrosion of distribution pipes, Environ. Pollut. 57 (2) (1989) 167–178, https://doi.org/10.1016/0269-7491(89)90008-0.
[6] X. Xu, R. Ray, Y. Gu, H.J. Ploehn, L. Gearheart, K. Raker, W.A. Scrivens, Electrophoretic analysis and purification of fluorescent single-walled carbon nanotube fragments, J. Am. Chem. Soc. 126 (40) (2004) 12736–12737, https://doi.org/10.1021/ja040082h.
[7] S.Y. Lim, W. Shen, Z. Gao, Carbon quantum dots and their applications, Chem. Soc. Rev. 44 (1) (2015) 362–381, https://doi.org/10.1039/c4cs00269e.
[8] S. Tao, S. Zhu, T. Feng, C. Xia, Y. Song, B. Yang, The polymeric characteristics and photoluminescence mechanism in polymer carbon dots: a review, Mater. Today Chem 6 (2017) 13–25, https://doi.org/10.1016/j.mtchem.2017.09.001.
[9] J. Liu, R. Li, B. Yang, Carbon dots: a new type of carbon-based nanomaterial with wide applications, ACS Cent. Sci. 6 (12) (2020) 2179–2195, https://doi.org/10.1021/acscentsci.0c01306.
[10] X. Sun, Y. Lei, Fluorescent carbon dots and their sensing applications, TrAC Trend. Anal. Chem. 89 (2017) 163–180, https://doi.org/10.1016/j.trac.2017.02.001.
[11] X. Sun, C. Brückner, Y. Lei, One-pot and ultrafast synthesis of nitrogen and phosphorus Co-doped carbon dots possessing bright dual wavelength fluorescence emission, Nanoscale 7 (41) (2015) 17278–17282, https://doi.org/10.1039/C5NR05549K.
[12] X. Sun, J. He, Y. Meng, L. Zhang, S. Zhang, X. Ma, S. Dey, J. Zhao, Y. Lei, Microwave-assisted ultrafast and facile synthesis of fluorescent carbon nanoparticles from a single precursor: preparation, characterization and their application for the highly selective detection of explosive picric acid, J. Mater. Chem. A 4 (11) (2016) 4161–4171, https://doi.org/10.1039/C5TA10027E.
[13] Z.L. Wu, Z.X. Liu, Y.H. Yuan, Carbon dots: materials, synthesis, properties and approaches to long-wavelength and multicolor emission, J. Mater. Chem. B 5 (21) (2017) 3794–3809, https://doi.org/10.1039/C7TB00363C.
[14] L. Pan, S. Sun, A. Zhang, K. Jiang, L. Zhang, C. Dong, Q. Huang, A. Wu, H. Lin, Truly fluorescent excitation-dependent carbon dots and their applications in multicolor cellular imaging and multidimensional sensing, Adv. Mater. 27 (47) (2015) 7782–7787, https://doi.org/10.1002/adma.201503821.
[15] K. Jiang, S. Sun, L. Zhang, Y. Lu, A. Wu, C. Cai, H. Lin, Red, green, and blue luminescence by carbon dots: full-color emission tuning and multicolor cellular imaging, Angew. Chem. Int. Ed. 54 (18) (2015) 5360–5363, https://doi.org/10.1002/anie.201501193.
[16] F. Yuan, Z. Wang, X. Li, Y. Li, Z. Tan, L. Fan, S. Yang, Bright multicolor bandgap fluorescent carbon quantum dots for electroluminescent light-emitting diodes, Adv. Mater. 29 (3) (2017), 1604436, https://doi.org/10.1002/adma.201604436.
[17] H. Ding, S.-B. Yu, J.-S. Wei, H.-M. Xiong, Full-color light-emitting carbon dots with a surface-state-controlled luminescence mechanism, ACS Nano 10 (1) (2016) 484–491, https://doi.org/10.1021/acsnano.5b05406.
[18] X. Ma, W. Zhong, J. Zhao, S.L. Suib, Y. Lei, "Self-heating" Enabled one-pot synthesis of fluorescent carbon dots, Eng. Sci. (2020), https://doi.org/10.30919/es8d805.
[19] L.M.T. Phan, T.X. Hoang, S. Cho, Fluorescent carbon dots for sensitive and rapid monitoring of intracellular ferrous ion, Biosensors 12 (1) (2022) 41, https://doi.org/10.3390/bios12010041.
[20] T. Chen, F. Yang, X. Wu, Y. Chen, G. Yang, A fluorescent and colorimetric probe of carbyne nanocrystals coated Au nanoparticles for selective and sensitive detection of ferrous ions, Carbon N Y 167 (2020) 196–201, https://doi.org/10.1016/j.carbon.2020.06.003.
[21] F. Molina-Holgado, R.C. Hider, A. Gaeta, R. Williams, P. Francis, Metals ions and neurodegeneration, BioMetals 20 (3–4) (2007) 639–654, https://doi.org/10.1007/s10534-006-9033-z.
[22] W. Zhu, Y. Liu, W. Wang, Z. Zhou, J. Gu, Z. Zhang, H. Sun, F. Liu, A paradox: Fe^{2+}-containing agents decreased ROS and apoptosis induced by CoNPs in vascular endothelial cells by inhibiting HIF-1α, Biosci. Rep. (1) (2021) 41, https://doi.org/10.1042/BSR20203456. BSR20203456.
[23] Y. Lu, G. Ruan, W. Du, J. Li, N. Yang, Q. Wu, L. Lu, C. Zhang, L. Li, Recent progress in rational design of fluorescent probes for Fe^{2+} and bioapplication, Dyes Pigment. 190 (2021), 109337, https://doi.org/10.1016/j.dyepig.2021.109337.
[24] K. Xiao, Z. Li, J. Song, Z. Bai, W. Xue, J. Wu, C. Dong, Effect of concentrations of Fe^{2+} and Fe^{3+} on the corrosion behavior of carbon steel in Cl^- and SO_4^{2-} aqueous environments, Met. Mater. Int. 27 (8) (2021) 2623–2633, https://doi.org/10.1007/s12540-019-00590-y.
[25] A. Saini, Z. Gatland, J. Begley, L. Kisley, Investigation of fluorophores for single-molecule detection of anodic corrosion redox reactions, MRS Commun. 11 (6) (2021) 804–810, https://doi.org/10.1557/s43579-021-00096-y.
[26] J.R. Lakowicz, Principles of Fluorescence Spectroscopy, 3rd Edition, Springer, 2006.
[27] S. Wei, L. Tan, X. Yin, R. Wang, X. Shan, Q. Chen, T. Li, X. Zhang, C. Jiang, G. Sun, A Sensitive "ON–OFF" fluorescent probe based on carbon dots for Fe^{2+} detection and cell imaging, Analyst 145 (6) (2020) 2357–2366, https://doi.org/10.1039/C9AN02309G.
[28] N. Gokulakrishnan, N. Kania, B. Léger, C. Lancelot, D. Grosso, E. Monflier, A. Ponchel, An ordered hydrophobic p6mm mesoporous carbon with graphitic pore walls and its application in aqueous catalysis, Carbon N Y 49 (4) (2011) 1290–1298, https://doi.org/10.1016/j.carbon.2010.11.048.
[29] M. Zhou, Z. Zhou, A. Gong, Y. Zhang, Q. Li, Synthesis of highly photoluminescent carbon dots via citric acid and tris for iron(III) ions sensors and bioimaging, Talanta 143 (2015) 107–113, https://doi.org/10.1016/j.talanta.2015.04.015.
[30] T.R. Gengenbach, G.H. Major, M.R. Linford, C.D. Easton, Practical guides for X-ray photoelectron spectroscopy (XPS): interpreting the carbon 1 s spectrum, J. Vac. Sci. Technol. A 39 (1) (2021), 013204, https://doi.org/10.1116/6.0000682.

[31] L. Wang, S.-.J. Zhu, H.-.Y. Wang, S.-.N. Qu, Y.-.L. Zhang, J.-.H. Zhang, Q.-.D. Chen, H.-.L. Xu, W. Han, B. Yang, H.-.B. Sun, Common origin of green luminescence in carbon nanodots and graphene quantum dots, ACS Nano 8 (3) (2014) 2541–2547, https://doi.org/10.1021/nn500368m.

[32] X. Gong, Q. Hu, M.C. Paau, Y. Zhang, S. Shuang, C. Dong, M.M.F. Choi, Red-green-blue fluorescent hollow carbon nanoparticles isolated from chromatographic fractions for cellular imaging, Nanoscale 6 (14) (2014) 8162–8170, https://doi.org/10.1039/C4NR01453G.

[33] W. Wang, Y. Li, L. Cheng, Z. Cao, W. Liu, Water-soluble and phosphorus-containing carbon dots with strong green fluorescence for cell labeling, J. Mater. Chem. B 2 (1) (2014) 46–48, https://doi.org/10.1039/C3TB21370F.

[34] A. Iqbal, Y. Tian, X. Wang, D. Gong, Y. Guo, K. Iqbal, Z. Wang, W. Liu, W. Qin, Carbon dots prepared by solid state method via citric acid and 1,10-phenanthroline for selective and sensing detection of Fe^{2+} and Fe^{3+}, Sens. Actuat. B Chem. 237 (2016) 408–415, https://doi.org/10.1016/j.snb.2016.06.126.

[35] S.J. Xiao, Z.J. Chu, J. Zuo, X.J. Zhao, C.Z. Huang, L. Zhang, Fluorescent carbon dots: facile synthesis at room temperature and its application for Fe^{2+} sensing, J. Nanoparticle Res. 19 (2) (2017) 84, https://doi.org/10.1007/s11051-016-3698-1.

[36] T. Prathumsuwan, S. Jamnongsong, S. Sampattavanich, P. Paoprasert, Preparation of carbon dots from succinic acid and glycerol as ferrous ion and hydrogen peroxide dual-mode sensors and for cell imaging, Opt. Mater. 86 (2018) 517–529, https://doi.org/10.1016/j.optmat.2018.10.054.

[37] L. Gao, D. Wu, W. Tan, F. Pan, J. Xu, Y. Tao, Y. Kong, A facile synthesis of two ionized fluorescent carbon dots and selective detection toward Fe^{2+} and Cu^{2+}, Nanoscale Adv. 2 (7) (2020) 2943–2949, https://doi.org/10.1039/D0NA00151A.

[38] J. Singh, S. Kaur, J. Lee, A. Mehta, S. Kumar, K.-.H. Kim, S. Basu, M. Rawat, Highly fluorescent carbon dots derived from mangifera indica leaves for selective detection of metal ions, Sci. Total Environ. 720 (2020), 137604, https://doi.org/10.1016/j.scitotenv.2020.137604.

[39] Y. Zhan, S. Yang, F. Luo, L. Guo, Y. Zeng, B. Qiu, Z. Lin, Emission wavelength switchable carbon dots combined with biomimetic inorganic nanozymes for a two-photon fluorescence immunoassay, ACS Appl. Mater. Interfaces 12 (27) (2020) 30085–30094, https://doi.org/10.1021/acsami.0c06240.

[40] H. Shah, Q. Xin, X. Jia, J.R. Gong, Single precursor-based luminescent nitrogen-doped carbon dots and their application for iron (III) sensing, Arab. J. Chem. 12 (7) (2019) 1083–1091, https://doi.org/10.1016/j.arabjc.2019.06.004.

[41] N. Preeyanka, M. Sarkar, Probing how various metal ions interact with the surface of QDs: implication of the interaction event on the photophysics of QDs, Langmuir 37 (23) (2021) 6995–7007, https://doi.org/10.1021/acs.langmuir.1c00548.

[42] X. Guo, J. Huang, M. Wang, L. Wang, A dual-emission water-soluble g-C_3N_4@AuNCs-based fluorescent probe for label-free and sensitive analysis of trace amounts of ferrous (II) and copper (II) ions, Sens. Actuat. B Chem. 309 (2020), 127766, https://doi.org/10.1016/j.snb.2020.127766.

[43] X. Wu, C. Ma, J. Liu, Y. Liu, S. Luo, M. Xu, P. Wu, W. Li, S. Liu, In situ green synthesis of nitrogen-doped carbon-dot-based room-temperature phosphorescent materials for visual iron ion detection, ACS Sustain. Chem. Eng. 7 (23) (2019) 18801–18809, https://doi.org/10.1021/acssuschemeng.9b03281.